A genomic perspective of metal-resistant bacteria from gold particles: Possible survival mechanisms during gold biogeochemical cycling

Santonu Kumar Sanyal[1,2], Frank Reith[1,2]† , and Jeremiah Shuster[1,2*]

Affiliations:

[1] School of Biological Sciences, The University of Adelaide, Adelaide, 5005 South Australia.

[2] CSIRO Land & Water, Glen Osmond, 5064, South Australia, Australia.

*Correspondence: Dr. Jeremiah Shuster

School of Biological Sciences, University of Adelaide, Adelaide, 5005, South Australia, Email: jeremiah.shuster@adelaide.edu.au

† Passed away prior to the completion of this study.

Number of Pages: 26

Number of Figures and Tables: 1 Graphical Abstract, 8 Figures, 3 Tables

Running title: Bacterial survival mechanisms during gold particle biotransformation

Abstract

A bacterial consortium was enriched from gold particles that 'experienced' ca. 80 years of biotransformation within waste-rock piles (Australia). This bacterial consortium was exposed to 10 µM $AuCl_3$ to obtain Au-tolerant bacteria. From these isolates, *Serratia* sp. and *Stenotrophomonas* sp. were the most Au-tolerant and reduced soluble Au as pure gold nanoparticles, indicating that passive mineralisation is a mechanism for mediating the toxic effect of soluble Au produced during particle dissolution. Genome-wide analysis demonstrated that these isolates also possessed various genes that could provide cellular

defence enabling survival under heavy-metal stressed condition by mediating the toxicity of heavy metals through active efflux/reduction. Diverse metal-resistant genes or genes clusters (*cop*, *cus*, *czc*, *znt*, *ars*) were detected, which could confer resistance to soluble Au. Comparative genome analysis revealed that the majority of detected heavy-metal resistant genes were similar (i.e. orthologous) to those genes of *Cupriavidus metallidurans* CH34. The detection of heavy-metal resistance, nutrient cycling, and biofilm formation genes (*pgaABCD*, *bsmA, hmpS)* may have indirect yet important roles when dealing with soluble Au during particle dissolution. In conclusion, the physiological and genomic results suggest that bacteria living on gold particles would likely use various genes to ensure survival during Au biogeochemical cycling.

Keywords: *Gold particles; Heavy-metal resistance; Serratia; Stenotrophomonas; Gold biogeochemistry, Gold biogeochemical cycling, Au-tolerant bacteria*

Introduction

Bacteria residing on gold particles have been directly observed using high-resolution electron microscopy or indirectly inferred using high-throughput molecular techniques (Rea *et al*. 2018; Reith *et al*. 2009; Shuster *et al*. 2015). From a materials characterisation perspective, the surface of particles often contained crevices that are filled with secondary gold structures (pure gold nanoparticles or bacteriomorphic structures), inorganic material (clays and other minerals), and organic material (cells and Extracellular Polymeric Substances, EPS) (**Fig. 1**). Crevices containing these materials are commonly referred to polymorphic layers and are considered microenvironments (or ecological micro-niches) where gold dissolution and gold precipitation are likely to occur, thereby forming secondary gold structures (Reith, Stewart L and Wakelin 2012b ; Shuster *et al*. 2015; Shuster et al.

2017; Youngson and Craw 1993). Studies taking a molecular approach have detected a number of bacterial operational taxonomical units (OTUs) from the direct amplification of 16S rDNA from gold particles (Reith *et al*. 2018 and references therein). It has been revealed that these OTUs represent a diverse range of bacteria, with various functional capabilities, that could form multispecies biofilms on gold particles (Rea, Zammit and Reith 2016). Hence, the notion that bacterial biofilms commonly occur on particles and contribute to biogeochemical conditions within the microenvironments (polymorphic layers) they inhabit (Reith *et al*. 2010; Reith *et al*. 2018). More specifically, the bacterial biochemical activities within the polymorphic layers could create a suitable physicochemical condition including low pH and organic ligands for gold dissolution from particles (Sanyal, Shuster and Reith 2019b).

Few studies have directly enriched or characterised viable bacteria that occur within polymorphic layers on gold particles or determined whether or not particle-associated bacteria are tolerant to soluble Au, i.e., gold that would be dissolved during the biotransformation of particles (Sanyal, Shuster and Reith 2019a; Shuster *et al*. 2015a; Sanyal *et al.* 2020). Additionally, studies on gold geomicrobiology have focused on the interactions of various photosynthetic or chemolithotrophic bacteria or low molecular weight compounds, i.e., amino acid, cyanide, protein, from proxy bacterial species with soluble auric thiosulphate or chloride (Johnston *et al*. 2013; Lengke *et al*. 2006; Lengke and Southam 2005; Shuster *et al*. 2014; Shuster *et a*l. 2015b; Southam and Beveridge 1994).

Microbes are known to catalyse the oxidation of metals (e.g., Mn, Fe, Cu, Ag, Au) under Earth's near-surface environmental conditions (Gadd 2010; Jelen, Giovannelli and Falkowski 2016). In terms of Au biogeochemical cycling, it has been suggested that bacteria/biofilms contribute to gold particle dissolution via the production of organic acids. Bacteria/biofilms complete the Au biogeochemical cycle by contributing to gold

precipitation. During passive mineralisation, bacteria/biofilms act as a reservoir of electrons that are "stripped" away by soluble Au which has a strong electron affinity (Shuster and Reith 2018). While gold biogeochemical cycling increases gold purity on the outer surface of particles, soluble Au is highly cytotoxic and can diffuse into the cytoplasm of cells, thereby generating oxidative stress and potentially inhibiting protein/enzyme function (Wiesemann *et al*. 2017; Zammit *et al*. 2016). Under these conditions, bacteria can become Au-tolerant and use different biochemical machinery to mediate the toxic effect of soluble Au. For example, *Cupriavidus metallidurans* CH34 is an aurophilic bacterium that is often detected on gold particles as well as in mineralised soils/sediment. This bacterium has been shown to express a gold/copper-regulated gene (*copA*) leading to the energy-dependent reduction and precipitation of soluble Au, i.e., active mineralisation. Additionally, *C. metallidurans* CH34 has been shown to express and up-regulate the oxidative stress-related genes in the presence of soluble Au (Bütof *et al*. 2018; Zammit et al. 2016).

In terms of linking particle-associated bacteria with Au biogeochemical cycling, previous studies have assigned broad putative functions, e.g., EPS production, auto-aggregation, C/N cycling, or cell dispersion, to OTUs representing bacteria on gold particles (Rea, Zammit and Reith 2016; Reith *et al*. 2018; Sanyal, Shuster and Reith 2019a). In doing so, the inferred presence of bacteria and their assigned putative functions were used to reconstruct multispecies 'biofilms' that could contribute to Au biogeochemical cycling on particles (Rea, Zammit and Reith 2016; Reith *et al*. 2018). More recently, functional capabilities were evaluated from bacterial DNA from gold particles obtained from various depositional environments around the world (Reith *et al*. 2019). Although viable Au-tolerant bacteria have been enriched from particles (Sanyal, Shuster and Reith 2019a), identification of their functional capabilities is a gap in the current literature. Therefore, the aim of this present study was to analyse the genome of metabolically active bacteria enriched from Au

particles. In doing so, Au-tolerant bacteria were isolated from particles and their physiological response to soluble Au stress was assessed. Additionally, their genomes were analysed to ascertain their likely functional capabilities that could be used as "survival mechanisms" during Au biogeochemical cycling. We hypothesize that Au-tolerant bacteria harbour diverse heavy-metal resistant genes similar to *C. metalidurans* CH34, which could enable survival during gold particle dissolution within polymorphic layers. To test the hypothesis, this study evaluates the soluble Au tolerance/reduction capacity of the Au-tolerant isolates as well as compares their genomes with the genome of *C. metallidurans* CH34. This study is a continuation of how Au biogeochemical cycling selects for Au-tolerant bacteria residing on particles undergoing biotransformation. More importantly, this study provides a physiological and genomic perspective of how these microbes adapt to "extreme" microenvironmental conditions.

Materials and Methods

Bacterial enrichment from gold particles

Waste-rock from an abandoned mine site in Donnybrook, Western Australia, was sluiced and panned to recover residual gold that occurred as particles. The environment, history of mining activity, sampling procedures, and gold particle structure and chemistry are fully described in Sanyal, Shuster and Reith (2019a) (doi: 10.1093/femsec/fiz078). For this study, a bacterial enrichment was obtained by placing 20 gold particles into a test tube with a push cap containing 20 mL of Tris Minimal Medium (TMM). Abiotic controls included test tubs with push caps containing: TMM or sterile saline solution (20 mL) with 20 gold particles. Note that all test tubes, push caps, TMM, and saline solutions were sterilised using an autoclave prior to experimental use. The bacterial enrichment and abiotic controls were placed in a 25 ˚C shaking (120 rpm) incubator for 14 days.

Selecting and identifying bacterial isolates with the highest Au-tolerance

To isolate Au-tolerant bacteria, an aliquot (1 mL) from the bacterial enrichment was transferred to a test tube containing 19 mL of fresh TMM with 10 µM $AuCl_3$. This selective enrichment was incubated for 7 days under the same conditions used for the primary enrichment. After incubation, the selective enrichment was serially diluted (10^{-3} fold) using filter sterilised (0.2 µm-size pore size) deionised water. The terminal dilution was transferred onto solid agar (1.5 $\%_{w/v}$) TMM with 10 µM $AuCl_3$. The plates were then placed in 25 °C incubator for 7 days. Individual bacterial colonies were first observed after 2 days of incubation. After 7 days of incubation, the most abundant colonies (5) that were morphologically distinct were selected, sub-cultured, and purified using fresh liquid TMM.

From the 5 isolates, genomic DNA was extracted using the ATP™ Genomic DNA Mini Kit (Promega, USA). To check whether or not any of the isolates contained any extra-chromosomal DNA, the Wizard®Plus SV Minipreps plasmid DNA Purification kit (Promega, USA) was used to extract any plasmid DNA. Using universal primers for the bacterial 16S rRNA gene (27F and 1492R), polymerase chain reaction (PCR) was performed followed by sequencing. Partial 16S rRNA gene sequences from individual isolates were subjected to nucleotide BLAST analysis (http://www.ncbi.nlm.nih.gov/) to identify the most similar species based on the most significant sequence homology. A phylogenetic tree was constructed using assembled sequences of 16S rRNA gene and the neighbour-joining algorithms following the p-distance model by using MEGA 5.0 software (Tamura *et al*. 2007). The 16S rRNA sequences of the respective isolates were deposited in National Centre for Biotechnology Information (NCBI) GenBank database under the accession numbers MN704661- MN704666. For this article, isolate notation has been simplified: D1 (reported as D2.2), D2 (D5.1), D3 (13.1), D4 (D10.1), and D5 (D11.1).

From the 5 bacterial isolates (D1 to D5), isolates with the highest Au-tolerance were selected for further genome-wide analysis. Using a 96 well microtiter plate, wells were filled with 20 µL of a pure bacterial culture and 130 µL of fresh TMM or TMM containing $AuCl_3$ (10, 25, or 50 µM Au final concentration). Both types of growth medium, with no bacterial inoculum, were also used as abiotic controls. All experiments and abiotic controls were performed in triplicate. The optical density of the wells was measured using a Synergy™ Mx Microplate Reader (BioTek); the average optical density (OD_{600}) of all wells was 0.04 ±0.02. The plate was placed in a 25 ºC incubator for 7 days. After incubation, bacterial growth was determined by re-measuring the OD using the same microplate reader. Wells with $OD_{600} \geq 0.2$ were considered to have positive bacterial growth, i.e., within the exponential growth stage.

Most Au-tolerant isolates: growth patterns and gold reduction capacity

Growth patterns: Since the D1 and D2 isolates were the most Au-tolerant, their growth patterns with and without the presence of $AuCl_3$ were assessed using an experiment that was performed in a similar manner as the Au-tolerance experiment described in Section 2.2. Using a 96 well microtiter plate, aliquots (20 µL) of D1 or D2 isolates were transferred to wells containing 130 µL of TMM or TMM supplemented with $AuCl_3$ (10, 25, or 50 µM Au final concentration). The plate was placed in a 25 ºC incubator for 5 days. Optical densities were measured using the same BioTek Synergy™ Mx Microplate Reader at 2 hour intervals (between 0 –18 hours of incubation), followed by 12-hour intervals (between 24 – 96 hours of incubation), and at 120 hours of incubation.

Au-reduction capacities: The D1 and D2 isolates were used to determine their respective capacity to reduce soluble Au. In doing so, sterile borosilicate glass test tubes containing a bacterial isolate (5 mL-volume) was exposed to $AuCl_3$ with a final measured concentration of 168 µM Au. These bacterial isolate-Au systems were covered with sterile

push caps and were mixed by vortex. Growth medium (pH 7.0 ±0.5) containing 200 µM Au was used as an abiotic control to determine if constituents in TMM could abiotically reduce Au. Additionally, 168 µM Au solutions were also used as abiotic controls to determine whether or not Au could abiotically precipitate out of solution during the course of the experiment. The bacterial isolate-Au systems and the abiotic controls were wrapped in aluminium foil to prevent any photocatalytic effects, performed in triplicate, and placed in a 25 ºC shaking incubator. Note that the 168 µM Au concentration was necessary for visualisation by electron microscopy (described below). The exposures to soluble Au were arrested after 0.5, 1, 2, 4, 8, or 16 hours of incubation by centrifuging (12,000 × *g* for 1 min) the bacterial isolate-Au systems to form a bacterial-gold pellet and removing the supernatant, i.e., spent TMM with residual soluble gold. The supernatants were separately filtered using 0.2 µm pore-size filters and were analysed using an Agilent 8900x Triple Quad Inductively Coupled Plasma-Mass Spectrometer (ICP-MS) to measure the concentration of residual (unreacted) soluble Au. The amount of reduced gold was calculated by subtracting the measured concentrations from the initial input.

The bacterial-gold pellets were immediately washed by resuspending the cells in phosphate-buffered saline (PBS, pH = 7.0) and mixing by vortex to rinse any soluble Au that may have been adsorbed on the extracellular surface of cells. The cells were re-pelleted by centrifugation, and the PBS supernatant was discarded. After performing a second wash in the same manner, the bacterial-gold pellets were resuspended in $2\%_{(aq)}$ glutaraldehyde for 24 hours to fix the cells.

Electron microscopy: Fixed cells from bacterial-gold pellets were prepared for scanning electron microscopy in the methods modified from Shuster et al. (2019a). Briefly, fixed cells were centrifuged (12,000 × *g* for 1 min) to form a pellet and the supernatant containing residual fixative was discarded. The bacterial-gold pellets were separately

dehydrated in a series of ethanol solutions ($70\%_{(aq)}$, $90\%_{(aq)}$, 3 × 100%), followed by a 1:1 ratio of 100% hexamethyldisilazane (HMDS):100% ethanol, and finally by 100% HMDS. The bacterial-gold pellets were separately incubated in each solution for 15 min. Dehydrated samples were collected onto 0.2 μm pore-size filters, air-dried for 24 hours, mounted onto aluminium stubs using carbon adhesive tabs, and coated with a 20 nm-thick deposition of carbon. The samples were characterised using secondary electron (SE) or backscatter electron (BSE) imaging modes using a Helios NanoLab Scanning Electron Microscope (SEM), equipped with an Oxford Instruments Energy Dispersive Spectrometer (EDS), operating at 5 kV or 10 kV accelerating voltage.

Additional bacterial-gold pellets were prepared for transmission electron microscopy. In doing so, the fixed cells were post-fixed using $2\%_{(aq)}$ osmium tetroxide followed by $1\%_{(aq)}$ uranyl acetate with 1 hour exposures for each solution. The post-fixed cells were then dehydrated in a serial ethanol series ($70\%_{(aq)}$, $90\%_{(aq)}$, $95\%_{(aq)}$, and 3 × 100%) with 15 min incubation for each concentration. The samples were then embedded in a 1:1 ratio of propylene oxide:epoxy resin and incubated for 1 hour. The samples were then transferred to 100% epoxy resin and were allowed to polymerise overnight on a rotating 70 °C heating block. From the polymerised resin block, ultrathin (70 nm-thick) sections were the cut using a diamond knife and a 4 Leica ultramicrotome, collected on formvar, carbon-coated copper grids, and analysed using a Phillips CM200 transmission electron microscope (TEM), equipped with GATAN 832 SC1000 CCD camera, operating at 200 kV.

Most Au-tolerant isolates: genomic capabilities

Genomic DNA from the D1 and D2 isolates was analysed at the molecular level to ascertain their genomic capabilities that could contribute to Au biogeochemical cycling. The genome sequencing was performed by using the Illumina HiSeq 2500 Sequencing System

(Illumina, Inc). The raw sequences were trimmed and filtered by using AdapterRemoval v.2 for removal of sequencing adaptor sequences and low-quality bases (Schubert , Lindgreen and Orlando 2016). The filtered sequence reads quality was examined by using FastQC (Andrews 2010). For sequence assembly, "Unicycler" assembly pipeline was used (Wick *et al*. 2017). Unicycler contains the SPAdes and PILON software to assemble sequence reads, resolve single nucleotide polymorphisms (SNPS), insertion-deletion (indels) or local mis-assemblies. The assembled contigs were re-arranged using Mauve, i.e., multiple genome alignments, to get ordered contigs (Darling *et al*. 2004). The contigs re-arrangement was performed using closest reference genomes available in the NCBI GenBank.

The functional annotation of the genomes was carried out using Patric (https://www.patricbrc.org/) and further processed in NCBI Prokaryotic Genome Annotation Pipeline (PGAP) (Wattam *et al*. 2013). The presence of genomic islands (GIs) in the genome of the isolates were detected by the prediction approach using islandviewer4 (Bertelli *et al*. 2017). Note that this tool incorporates the IslandPick, IslandPath, DIMOB and SIGI-HMM algorithms. Additionally, the presence of transposable elements (i.e., insertion sequence, IS) were detected in the genomes using ISsaga2 (https://www-is.biotoul.fr/). This Whole Genome Shotgun (WGS) project has been deposited at NCBI GenBank under the accession SRHZ00000000 (*Serratia* sp.) and SRIA00000000 (*Stentrophomonas* sp.). The version (SRHZ01000000 and SRIA01000000) described in this paper is statistically validated by NCBI and available on NCBI website.

Comparative Genomics

The genome sequences of the two Au-tolerant isolates were compared with the genome of *C. metallidurans* CH34. In doing so, the genome sequence of *C. metallidurans* CH34 was obtained from the National Centre for Biotechnology Information (NCBI) genome

sequence repository (https://www.ncbi.nlm.nih.gov/genome/). The genome-wide comparison and annotation of clusters of orthologous groups (COGs) between organisms were performed using the OrthoVenn2 (Xu *et al.* 2019). Additionally, MEGA 5.2 was used for comparative analysis of orthologous gene sequences to understand the extent of sequence homology. Note that this analysis was exclusively performed to target those genes responsible for heavy-metals resistance, nutrient cycling (i.e., carbon/nitrogen metabolism in nutrient limiting condition), stress response, and biofilm formation.

Results

Bacterial enrichments from gold particles

Positive growth in the bacterial enrichment was observed by the progressive development of turbidity during incubation. Turbidity was first observed after 7 days and was attributed to bacterial cells, which was confirmed by using 10 mL-volume aliquots of the fluid phase and a light microscopy (data not shown). Turbidity did not occur in the abiotic controls.

Selective enrichment and isolation of Au-tolerant bacteria

Some bacteria, transferred from the primary enrichment, were able to grow in the presence of 10 µM $AuCl_3$. From this selective enrichment, 5 morphologically distinct colonies (D1 to 5) were isolated. Sequencing and phylogenetic reconstruction of 16S rRNA gene revealed that 4 out of 5 isolates, at the phylum level, belonged to Proteobacteria while one isolate belonged to Actinobacteria. The 5 isolates were identified as *Serratia* sp. (D1), *Stenotrophomonas* sp. (D2), *Pseudomonas* sp. (D3), *Arthrobacter* sp. (D4), and *Enterobacter* sp. (D5) (**Fig. 2**). *Serratia* sp. (D1) and *Stenotrophomonas* sp. (D2) were the most tolerant to soluble Au as they were able to grow in the presence of 50 and 25 µM $AuCl_3$, respectively.

Comparatively, *Pseudomonas* sp. (D3), *Arthrobacter* sp. (D4), and *Enterobacter* sp. (D5) were the least tolerant to soluble Au as growth only occurred in the presence of 10 µM $AuCl_3$.

Serratia sp. and Stenotrophomonas sp.: growth patterns and Au-reduction capacity

When grown in TMM, *Serratia* sp. and *Stenotrophomonas* sp. reached a stationary growth phase ($OD_{600} \simeq 0.6$) within 48 hours of incubation at 25 ºC and demonstrated a 'normal' growth pattern. When *Serratia* sp. and *Stenotrophomonas* sp. were grown in the presence of soluble Au, lag-phases were prolonged, and the stationary growth phase began between 100 and 120 hours of incubation (**Fig. 3**).

The reduction of soluble Au by *Serratia* sp. and *Stenotrophomonas* sp. was rapid; almost 50% of soluble was reduced within 30 minutes by both isolates. After 4 hours of exposure, both isolates reduced ≥89% of $AuCl_3$ and appeared to reach a maximum reduction capacity as the amount of Au in solution remained relatively similar after 8 and 16 hours (**Fig. 4A**). Note that Au concentrations in the abiotic controls did not change. Both *Serratia* sp. and *Stenotrophomonas* sp. reduced soluble Au as pure gold nanoparticles (euhedral crystals or octahedral platelets) that were less than 100 nm in size (**Fig. 4B-D**). While some gold nanoparticles occurred on the extracellular surface, TEM analysis demonstrated that some gold nanoparticles also occurred intracellularly (**Fig. 4E**).

Genome characterisation and comparative genomics

The (draft) genome of *Serratia* sp. and *Stenotrophomonas* sp. were approximately 5.2 Mb and 4.6 Mb in size with a guanine-cytosine (GC) content of 54.9% and 66.0%, respectively. The draft genome of *Serratia* sp. was assembled into 35 contigs containing 4771 functional genes, 55 pseudogenes and 27 frameshifted genes. Whereas the draft genome of

Stenotrophomonas sp. was assembled into 91 contigs containing 4176 functional genes, 46 pseudogenes and 14 frameshifted genes. For comparison, the genome organisation of *C. metallidurans* CH34 is different from these two isolates. It contains two large replicons (CHR 1 and 2) with a size of 3.93 Mb and 2.58 Mb, respectively (Janssen *et al.* 2010). It has been suggested that, the smaller replicon CHR2 might be acquired as a plasmid and later gradually evolved into a second chromosome (CHR1) through lateral gene transfer.

Both Au-tolerant isolates did not contain any plasmids, while CH34 contains two mega-plasmids. An interesting feature of *C. metallidurans* CH34 genome is the presence of laterally acquired genomic islands (total 16; 11 in CHR1) and the high abundance of transposable elements. The bioinformatical analysis of the genome of Au-tolerant isolates *Serratia* sp. and *Stenotrophomonas* sp. revealed that both isolates contain laterally acquired genomic islands (GIs) and the transposable elements. Using islandviewer4.0 tool, 6 GIs were detected in *Serratia* sp. D1 and 9 in *Stenotrophomonas* sp. D2. See **Table 1**, NCBI Accession PRJNA529743 (https://www.ncbi.nlm.nih.gov/bioproject/PRJNA529743) for further details regarding genome statistics for each isolate.

The genome-wide comparison of *Serratia* sp., *Stenotrophomonas* sp., and *C. metallidurans* CH34 demonstrated that *Stenotrophomonas* sp. and *C. metallidurans* CH34 shared 1511 orthologous gene clusters, whereas *Serratia* sp. and *C. metallidurans* CH34 shared 1675 gene clusters. Both Au-tolerant isolates, shared 1470 orthologous genes clusters. Interestingly, 1121 orthologous genes clusters were shared by all three isolates (**Fig. 5A**). These genes were involved in functioning with hydrolase, transporter, molecular function, oxidoreductase, transferase, cofactor binding, nucleotide binding, peptidase, etc activities (**Fig. 5B**).

Genes: Heavy-metal resistance, stress tolerance, nutrient cycling and biofilm formation

A total of 47 genes related to heavy-metal resistance (22), stress tolerance (10), nutrient cycling (9), or biofilm formation (6) were identified from *Serratia* sp. and *Stenotrophomonas* sp. Both isolates contained various genes clusters as well as distinct genes that covered a broad range of heavy metals (Cu, Pb, Co, Zn, Cd, As, and Cr) resistance **(Table 2)**. The orthologous clusters of copper-resistant genes of *Stenotrophomas* sp. (*copB, copD, cueO)* and *Serratia* sp. *(cusFCBA)* demonstrated significant sequence homology with the *cop* and *cus* genes of *C. metallidurans* CH34 (**Fig. 6**, **Table. 2**). *Serratia* sp. contained a Zn/Cd translocating P-type ATPase gene *zntA* while *Stenotrophomonas* sp. contained two sets of efflux-RND pump encoding *czcABC* genes clusters (**Fig.7**). Structurally and functionally similar *zntA* and *czcABC* genes were also detected in the genome of CH34 (**Fig. 7, Table 2**)

While *Serratia* sp. had more stress-response genes (10) compared to *Stenotrophomonas* sp. (6), all genes were related to neutralisation of free radicals causing cellular oxidative stress or damage, as well as metabolic or environmental stress. Among these stress tolerance genes, *gstA* (glutathione peroxidase), *gpx* (glutathione peroxidase), *sodB* (superoxide dismutase) and *ohr* (peroxide resistance) genes were detected in *Serratia* sp., *Stenotrophomonas* sp. and *C. metallidurans* CH34. In terms of nutrient cycling, genes for carbon, nitrogen, and xenobiotic compound metabolism under nutrient-limiting conditions were similar between the two isolates. Interestingly, all genes related to biofilm formation were distinct to each isolate. See **Table. 3** for the full list and descriptions of the stress tolerance, nutrient cycling, and biofilm formation genes detected in two isolates.

Discussion

Au-tolerant bacteria identification and gold mineralisation

Gold particles, including those from Donnybrook (**Fig. 1**), often contain pure gold nanoparticles or overgrowth depending on the degree of (bio)transformation (Groen, Craig and Rimstidt 1990; Rea *et al*. 2019; Sanyal, Shuster and Reith 2019; Youngson and Craw 1993). Nanoparticles form when gold-silver alloy is dissolved from a particle and soluble Au is reduced by an (in)organic substance (Shuster *et al*. 2017). In this present study, the selective enrichment of Au-tolerant bacteria supports the notion that gold dissolved from particles could selects for Au-tolerant bacteria (Reith *et al*. 2009; Sanyal, Shuster and Reith 2019). Viable Proteobacteria (*Shewanella* sp. and *Nitrobacter* sp.) on placer gold particles were thought to contribute to particle biotransformation within the Saldaña River, Colombia (Shuster *et al*. 2015a). Additionally, it has been demonstrated that *Stenotrophomonas* sp. and *Pseudomonas* sp. are capable of reducing soluble Au as nanoparticles (Karthikeyan and Beveridge 2002; Song *et al*. 2008); while EPS produced by *Serratia* sp. and *Arthrobacter* sp. can reduce heavy metals via passive biomineralisation (Shuhong *et al*. 2014; Srivastava and Thakur 2012). Therefore, it is reasonable to suggest that Au-tolerant Proteobacteria (*Serratia* sp., *Stenotrophomonas* sp., *Pseudomonas* sp., *Enterobacter* sp.) and Actinobacteria (*Arthrobacter* sp.), isolated in this study (**Fig. 2, 3**), could contributed to particle biotransformation within the waste-rock piles at Donnybrook. Additionally, the formation of octahedral gold platelets by *Serratia* sp. and *Stenotrophomonas* sp. appeared morphological similar to those which were observed on particles (compare **Fig. 4** and **1**). Therefore, it is possible that some octahedral gold platelets on particles could have been bacterially formed. Furthermore, the isolation of *Enterobacter* sp. highlights the diversity of Au-tolerant microbes on particles as this enteric bacterium has also been detected in wallabies and

kangaroos faeces (Gordon and FitzGibbon 1999; Hernández, Mellado and Martínez 1998). It is important to remember that mining activity ceased over 80 years ago, and the abandoned sites have been reclaimed by indigenous plants such as *Eucalyptus* sp. and *Allocasuarina* sp. and fauna (based on field observations). Therefore, this historic mining site is changing from an engineered environment to a natural environment. In doing so, enteric bacterium from animals could become incorporated into the microbial community of gold-bearing soils/sediments, thereby contributing to Au biogeochemical cycling.

Heavy-metal resistance genes

Gold particle dissolution likely occurs as punctuated "episodes" that reflect changes in seasonal to decadal rainfall patterns within a given environment (Shuster *et al*. 2017). In Donnybrook, particle dissolution likely occurred at a rate of 1.60×10^{-9} M Au per year within the waste-rock piles (Sanyal, Shuster and Reith 2019). During particle dissolution, soluble Au could form organic or inorganic Au complexes (Shuster and Reith 2018). If these soluble Au complexes are stable, sublethal concentrations could select for metal-tolerant bacteria residing on particles (Reith *et al*. 2009). Consequently, these metal-tolerant bacteria could contribute to Au biogeochemical cycling within microenvironments, i.e., polymorphic layers, thereby perpetuating the biotransformation of particles (Rea *et al*. 2018). In this study, the enrichment and isolation of Au-tolerant isolates from particles supports the notion that particle transformation selectively enriches heavy-metal resistant bacteria. The genome wide analysis and comparison of *Serratia* sp. and *Stenotrophomonas sp*. with each other and with *C. metallidurans* provides insight into the genome structure, genes, and biochemical function of these bacteria (**Fig. 5A, Table 1**). The presence of 1121 shared orthologous genes clusters between *Serratia* sp., *Stenotrophomonas* sp., and *C. metallidurans* CH34 highlights the functional similarity of the genomes of heavy-metal resistant bacteria (**Fig. 5A, B**). More-

importantly, the presence of various genomic islands and mobile genetic elements within the genome of Au-tolerant isolates highlights the possibility of lateral gene transfer between bacterial communities inhabiting Au particles. While further studies are required, laterally acquired genes could be essential for Au-tolerance in natural or engineered environments (Sanyal *et al.* 2020).

In this study, the detected copper-resistance genes clusters, e.g., *cop, cue, cus,* detected in the genome of Au-tolerant isolates were similar to those of *C. metallidurans* CH34 **(Fig. 6)**. Wiesemann et al. (2013) observed that the *copABCD* determinant on chromosome 2 of *C. metallidurans* CH34, which encodes periplasmic proteins involved in copper resistance, is necessary for the complete resistance against soluble Au. While this role primarily depends on the metabolic state of cells and Au/Cu concentration (Wiesemann et al. 2013), periplasmic copper oxidase (CueO) in association with CopA can inhibit the entry of soluble Au into the cytoplasm causing oxidative damage. Therefore, detoxification is achieved by reducing soluble Au as nanoparticles in the periplasmic space (Bütof *et al*. 2018). *Serratia* sp. and *Stenotrophomonas* sp. are generally considered to be more ubiquitous in soils/sediments and abundant on gold particles relative to *Cupriavidus* sp. (Adegoke, Stenström and Okoh 2017; Diels *et al*. 2009; Martínez *et al*. 2018). Therefore, the detection of similar copper-resistant genes (*copA, copCD, cueO)* in Au-tolerant *Serratia* sp. and *Stenotrophomonas* sp. suggests that these microbes could also synergistically detoxify soluble Au and Cu, even though they are not considered to be "aurophillic" microbes. Additionally, the presence of *copL and copB genes* in *Stenotrophomonas* sp., which are known to provide hyper-tolerance to Cu complexes in some metal-resistant bacteria along with *C. metallidurans* CH34, reflects the potential of periodic elevation of copper levels in the environment over the last 100 years and its effect on biosphere (Staehlin *et al.* 2016; Rosario-Cruz *et al*. 2019). It is important to note that particles from Donnybrook were

composed of 68.3 wt.% Au and 31.7 wt.% Ag (Sanyal, Shuster and Reith 2019a). Therefore, the presence of tripartite RND Cu/Ag efflux pump encoding genes, e.g., *cusFCBA*, in *Serratia* sp. highlights the possibility of Ag resistance in this isolate.

Other heavy-metal genes have been detected from bacterial consortia in soils associated with mineralised systems (Reith *et al*. 2012a). In this present study, other heavy metal (arsenic, cadmium, chromium, cobalt, zinc, and other copper) resistance gene/s (*znt*, *czc*, *ars*, *chr*) were detected in the genome of Au-tolerant bacteria. (**Table 2**). It is important to note that these heavy metals were also detected in elevated concentration in the gold-bearing host sediment (Sanyal, Shuster and Reith 2019a). *Stenotrophomonas* sp. contains two variants (distinct copy) of cobalt, zinc, cadmium specific RND efflux pump genes, i.e., *czcCBA* homologous to *C. metallidurans* **(Fig. 7**). Although these heavy-metal resistant genes were distinct to their respective Au-tolerant isolates, they could have important roles in bacterial survival, especially in a mineralised system containing elevated concentrations of other heavy-metals. More importantly, the presence of diverse heavy-metal resistance genes indicate that different metal-resistance genes could be expressed within Au-tolerant bacteria, thereby providing a broad-spectrum of metal-tolerance as a strategy for survival during particle biotransformation. Previous studies have primarily relied on a culture-independent approach to infer putative bacterial functions and their possible contribution to particle biotransformation (Rea *et al*. 2018; Rea, Zammit and Reith 2016; Reith *et al*. 2018). This present study provides genomic evidence of heavy-metal resistance from Au-tolerant bacteria isolated from gold particles.

General-stress response, nutrient cycling, and biofilm formation genes

Although general-stress genes are often non-specific, they can be categorised as responses to environmental, oxidative, or metabolic stress (Marles-Wright and Lewis 2007).

Interestingly, the majority of stress response genes detected from both Au-tolerant isolates code for oxidative stress mediating proteins (**Table 3**). These proteins are known to repair cellular damage caused by heavy metals, provide antioxidative defence, and metal homeostasis (Cabiscol, Tamarit Sumalla and Ros Salvador 2000). From both Au-tolerant isolates, oxidative-stress genes such as *gpx, gstA,, sodB, ohr* were detected and are important for repairing cellular damage attributed to heavy metals (Hu *et al*. 2005). More importantly, these genes were also detected in the genome of *C. metallidurans* CH34. The glutathione ABC transporter genes (*gsiBC*) was detected in the genome of *Serratia* sp.; the protein from this gene enables resistance against various heavy metals such as uranium, chromium, and cadmium (Yung *et al*. 2014). It is important to note that glutathione (GSH) can perform diverse functions including metal-ion chelation and protection against oxidative damage attributed to heavy-metal stress (Jozefczak *et al*. 2012). Additionally, it has been proposed that the reducing conditions and the presence of several glutathione-bearing proteins could destabilise and reduce soluble Au as pure gold nanoparticles (Bütof *et al*. 2018).

Since mining activity often involves stripping land of natural vegetation, i.e., disrupts natural environmental conditions, nutrient availability becomes an increasing important factor for successful reclamation (Salomons 1995; Stehouwer, Day and Macneal 2006; Tordoff, Baker and Willis 2000). Despite bushland re-establishment at Donnybrook, the waste-rock piles contained low total carbon and nitrogen concentrations (0.12 and 0.01 wt%, respectively; Sanyal et al., 2019a), which were consistent with other historic mining sites in semi-arid regions of Australia (Holt 1997; Reith and McPhail 2007). Polymorphic layers on gold particles, could be considered “extreme” in the context of limited nutrient availability. Therefore, it would be advantageous for Au-tolerant bacteria residing on particles to have genetic determinants for survival in these nutrient-deficient and heavy metal-bearing microenvironments. In terms of survival under carbon- or nitrogen-limiting conditions,

Serratia sp. and *Stenotrophomonas* sp. both contained carbon-storage regulator A gene (*csrA*) and a carbon-starvation gene (*cstA*) (**Table 3**). The former gene regulates central-carbon flux during nutrient-limiting conditions (Webb, Givskov and Kjelleberg 2003) while the latter gene metabolises peptides as a nutrient scavenging mechanism (Dubey *et al*. 2003). Additionally, both isolates contained nitrogen-regulation (*ntr*), nitrogen-assimilation (*nac*) genes and xenobiotic compound metabolising genes (**Table 3**), which enables bacteria to utilise a wide range of alternative nutrient sources (Merrick and Edwards 1995).

The expression of broad heavy-metal resistant genes or oxidative-stress genes provides instant protection ensuring survival of individual bacterial cells (De Angelis and Gobbetti 2004; Nies 1999). Biofilm formation, however, could be considered a long-term survival strategy, especially for communities that are exposed to soluble metals including Au since intracellular material from lysed cells can act as reductants for soluble metals (Harrison , Ceri and Turner 2007). A biofilm's matrix contains polysaccharides, which have been reported to bind heavy metal cations (Teitzel and Parsek 2003). With the oxidation of EPS material or cells at the biofilm-fluid interface, soluble Au 'strips' electrons allowing cells deeper within the biofilms to be protected from the toxic effect of soluble Au, thereby enabling survival (Karthikeyan and Beveridge 2002; Shuster *et al.* 2015b). In this study, *Serratia* sp. contained lipo-protein gene (*bsmA*) and biofilm formation regulator gene (*hmsP*); while, *Stenotrophomonas* sp. contained poly-β-1,6-N-acetyl-d-glucosamine export protein gene cluster (*pgaABCD*). Expression of these genes could help the respective bacteria to form and regulate biofilm development and provide biofilm structural integrity (Wang , Preston and Romeo 2004).

Outlook on gene expression

Given the importance of heavy-metal genes as well as other genes (general-stress response, nutrient-cycling, biofilm formation) as survival mechanisms during particle biotransformation, it is worth considering the possible timing of gene expression (**Fig. 8**). From this study, *Serratia* sp. and *Stenotrophomonas* sp. represent two Au-tolerant bacteria from a dominant phylum (Gamma-Proteobacteria) that reside on gold particles and could contribute to particle biotransformation. As such, the timing of gene expression is important, especially since microenvironmental conditions are dynamic and the punctuated episodes of gold dissolution with subsequent precipitation, i.e., cycling, likely reflects variations in seasonal or decade precipitation (Sanyal, Shuster and Reith 2019a; Shuster *et al*. 2017). Hence, water is necessary not only for gold-oxidation/-reduction reactions but also to support microbial life. Indeed, factors such as temperature, salinity, and pH would also be influenced by rainfall and would thereby influence Au biogeochemical cycling (Shuster and Reith 2018). When Au-tolerant bacteria are exposed to soluble Au during particle dissolution, it is possible that oxidative-stress genes could be expressed prior to the expression of heavy-metal resistance genes. This sequence of gene expression has been demonstrated using *Acidithiobacillus ferrooxidans* with an immediate exposure (pulse) to Cd^{2+} as well as a Cd-tolerant *A. ferrooxidans* cultured in the presence of soluble Cd (Ramos-Zúñiga *et al*. 2019). Therefore, it is possible that the contemporaneous expression of heavy-metal stress genes and oxidative-stress (attributed to heavy metals) genes could deal with the toxicity of soluble Au complexes. Furthermore, surface runoff into a river system can 'wash in' nutrients that are could support microbial growth within river sediment (Varol and Şen 2012), including biofilm formation on gold particles. Increased biofilm development would produce low molecular weight organic acids that could dissolve gold (and presumably silver) from

particles (Sanyal, Shuster and Reith 2019b). Under these conditions, cells would likely turn on gene expression to replace biomass "lost" to soluble Au reduction at the biofilm-fluid interface. While biofilm formation could promote gold particle dissolution, an increased amount of biomass (cells and EPS) could also favour passive gold mineralisation, thereby contributing to the continuum of Au biogeochemical cycling on particles.

Conclusion

The present study provides an in-depth analysis of physiological and molecular responses of Au-tolerant bacteria (*Serratia* sp. and *Stenotrophomonas* sp.) that naturally occur on the surface of gold particles. The exposure of *Serratia* sp. or *Stenotrophomonas* sp. to soluble Au was a laboratory-model representing how these bacteria would respond to gold dissolution during the biotransformation of particles within the waste-rock piles at Donnybrook (Western Australia). From a physiological perspective, these microbes were tolerant to high soluble Au concentrations (25 or 50 μM Au), which are considered anomalous relative to concentrations detected in mineralised systems. The viability of these isolates under this heavy-metal stressed conditions can be attributed, in part, to their ability to form gold nanoparticles either intracellularly or extracellularly, thereby reducing the toxicity of soluble Au. From a molecular perspective, these Au-tolerant isolates contained diverse heavy-metal resistance and stress tolerance genes similar to those of aurophilic *C. metallidurans* CH34. While the expression of these genes may have a role in Au particle biotransformation, their contributions to the genome of both isolates highlight the diversity of possible survival mechanisms in microenvironment (polymorphic layers) where Au biogeochemical cycling would likely occur. From a broad microbial ecology perspective, this study provides definitive biomolecular evidence of how these particle-associated bacteria

respond to changes within the microenvironments they inhabit; specifically, how these metal-resistant bacteria could survive during Au biogeochemical cycling.

Acknowledgments

In memory of Frank Reith – our dear friend, mentor, and colleague. His passion for research and sharing the joy of science and discovery will be cherished by his students, postdoctoral fellows, and collaborators. Funding for this research was made possible by the Australian Research Council Future Fellowship (ARC-FT100150200). Electron microscopy and microanalysis were performed at Adelaide Microscopy, an Australian Microscopy, and Microanalysis Research Facility. Authors would like to thank S.M. Pederson, A. Basak, K. Neubauer, and T. Reith for their technical support. The authors also thank the editor and reviewers for their constructive feedback.

Conflicts of interest

The authors declare no conflict of interest.

References

Adegoke AA, Stenström TA, Okoh AI. Stenotrophomonas maltophilia as an emerging ubiquitous pathogen: looking beyond contemporary antibiotic therapy. *Front Microbio*l 2017;**8**: 2276.

Andrews S. FastQC: a quality control tool for high throughput sequence data: Babraham Bioinformatics, Babraham Institute, Cambridge, United Kingdom, 2010.

Bertelli C, Laird MR, Williams KP et al. IslandViewer 4: expanded prediction of genomic islands for larger-scale datasets. *Nucleic Acids Res* 2017;**45**: W30-W5.

Bütof L, Wiesemann N, Herzberg M *et al.* Synergistic gold–copper detoxification at the core of gold biomineralisation in *Cupriavidus metallidurans*. *Metallomics* 2018;**10**:278–86.

Cabiscol Català E, Tamarit Sumalla J, Ros Salvador J. Oxidative stress in bacteria and protein damage by reactive oxygen species. *Int Microbiol.* 2000;**3(1)**:3-8. .

Darling AC, Mau B, Blattner FR *et al.* Mauve: multiple alignment of conserved genomic sequence with rearrangements. *Genome Res* 2004;**14**: 1394-403.

De Angelis M, Gobbetti M. Environmental stress responses in *Lactobacillus*: a review. *Proteomics.* 2004;**4**:106-122. doi:10.1002/pmic.200300497

Diels L, Van Roy S, Taghavi S *et al.* From industrial sites to environmental applications with Cupriavidus metallidurans. *Antonie van Leeuwenhoek* 2009;**96**: 247-58.

Dubey AK, Baker CS, Suzuki K *et al.* CsrA regulates translation of the *Escherichia coli* carbon starvation gene, cstA, by blocking ribosome access to the cstA transcript. *J Bacteriol* 2003;**185**: 4450-60.

Fairbrother L, Shapter J, Brugger J *et al.* Effect of the cyanide-producing bacterium *Chromobacterium violaceum* on ultraflat Au surfaces. *Chem Geol* 2009;**265**: 313-20.

Gadd GM. Metals, minerals and microbes: geomicrobiology and bioremediation. *Microbiology* 2010;**156**: 609-43.

Gordon DM, FitzGibbon F. The distribution of enteric bacteria from Australian mammals: host and geographical effects. *Microbiology* 1999;**145**: 2663-71.

Groen JC, Craig JR, Rimstidt JD. Gold-rich rim formation on electrum grains in placers. *Can Mineral* 1990;**28**: 207-28.

Harrison JJ, Ceri H, Turner RJ. Multimetal resistance and tolerance in microbial biofilms. *Nat Rev Microbiol* 2007;**5**: 928-38.

Hernández A, Mellado RP, Martínez JL. Metal Accumulation and Vanadium-Induced Multidrug Resistance by Environmental Isolates of *Escherichia hermannii* and *Enterobacter cloacae*. *Appl Environ Microbiol* 1998;**64**: 4317-20.

Holt JA. Grazing pressure and soil carbon, microbial biomass and enzyme activities in semi-arid northeastern Australia. *Appl Soil Ecol* 1997;**5**: 143-9.

Hu P, Brodie EL, Suzuki Y *et al.* Whole-genome transcriptional analysis of heavy metal stresses in Caulobacter crescentus. *J Bacteriol* 2005;**187**: 8437-49.

Janssen PJ, Van Houdt R, Moors H et al. The complete genome sequence of *Cupriavidus metallidurans* strain CH34, a master survivalist in harsh and anthropogenic environments. *PLoS One* 2010;5.

Jelen BI, Giovannelli D, Falkowski PG. The Role of Microbial Electron Transfer in the Coevolution of the Biosphere and Geosphere. *Annu Rev Microbiol* 2016;**70**: 45-62.

Johnston CW, Wyatt MA, Li X *et al.* Gold biomineralization by a metallophore from a gold-associated microbe. *Nat Chem Biol* 2013;**9**: 241-3.

Jozefczak M, Remans T, Vangronsveld J *et al.* Glutathione is a key player in metal-induced oxidative stress defenses. *Int J Mol Sci* 2012;**13**: 3145-75.

Karthikeyan S, Beveridge T. *Pseudomonas aeruginosa* biofilms react with and precipitate toxic soluble gold. *Environ Microbiol* 2002;**4**: 667-75.

Lengke MF, Ravel B, Fleet ME *et al.* Mechanisms of gold bioaccumulation by filamentous cyanobacteria from gold (III)− chloride complex. *Environ Sci Technol* 2006;**40**: 6304-9.

Lengke MF, Southam G. The effect of thiosulfate-oxidizing bacteria on the stability of the gold-thiosulfate complex. *Geochim Cosmochim Acta* 2005;**69**: 3759-72.

Marles-Wright J, Lewis R. Stress responses of bacteria. *Curr Opin Struct Biol* 2007;**17**: 755-60.

Martínez OA, Encina C, Tomckowiack C *et al. Serratia* strains isolated from the rhizosphere of raulí (*Nothofagus alpina*) in volcanic soils harbour PGPR mechanisms and promote raulí plantlet growth. *J Soil Sci Plant Nutr 2*018;**18**: 804-19.

Merrick M, Edwards R. Nitrogen control in bacteria. *Microbiol Mol Biol Rev* 1995;**59**: 604-22.

Nies DH. Microbial heavy-metal resistance. *Appl Microbiol Biotechnol* 1999;**51**: 730-50.

Ramos-Zúñiga J, Gallardo S, Martínez-Bussenius C *et al.* Response of the biomining *Acidithiobacillus ferrooxidans* to high cadmium concentrations. *J Proteomics* 2019;**198**: 132-44.

Rea MA, Standish CD, Shuster J *et al.* Progressive biogeochemical transformation of placer gold particles drives compositional changes in associated biofilm communities. *FEMS Microbiol Ecol* 2018;**94**: fiy080.

Rea MA, Zammit CM, Reith F. Bacterial biofilms on gold grains-implications for geomicrobial transformations of gold. *FEMS Microbiol Ecol* 2016;**92**: fiw082.

Rea MAD, Wulser P-A, Brugger J *et al.* Effect of physical and biogeochemical factors on placer gold transformation in mountainous landscapes of Switzerland. *Gondwana Res* 2019;**66**: 77-92.

Reith F, Brugger J, Zammit CM *et al.* Influence of geogenic factors on microbial communities in metallogenic Australian soils. *ISME J* 2012a;**6**: 2107.

Reith F, Etschmann B, Grosse C *et al.* Mechanisms of gold biomineralization in the bacterium *Cupriavidus metallidurans*. *Proc Natl Acad Sci USA*. 2009;**106**: 17757-62.

Reith F, Fairbrother L, Nolze G *et al.* Nanoparticle factories: Biofilms hold the key to gold dispersion and nugget formation. *Geology* 2010;**38**: 843-6.

Reith F, Falconer DM, Van Nostrand J *et al.* Functional capabilities of bacterial biofilms on gold particles. *FEMS Microbiol Ecol* 2019; **96**:fiz196.

Reith F, McPhail D. Mobility and microbially mediated mobilization of gold and arsenic in soils from two gold mines in semi-arid and tropical Australia. *Geochim Cosmochim Acta* 2007;**71**: 1183-96.

Reith F, Rea MAD, Sawley P *et al.* Biogeochemical cycling of gold: Transforming gold particles from arctic Finland. *Chem Geol* 2018;**483**: 511-29.

Reith F, Stewart L, Wakelin SA. Supergene gold transformation: Secondary and nano-particulate gold from southern New Zealand. *Chem Geol* 2012b;**320-321**: 32-45.

Rosario-Cruz Z, Eletsky A, Daigham NS et al. The copBL operon protects Staphylococcus aureus from copper toxicity: CopL is an extracellular membrane–associated copper-binding protein. *J Biol Chem* 2019;**294**: 4027-44.

Salomons W. Environmental impact of metals derived from mining activities: processes, predictions, prevention. *J Geochem Explor* 1995;**52**: 5-23.

Sanyal SK, Shuster J, Reith F. Biogeochemical gold cycling selects metal-resistant bacteria that promote gold particle transformation. *FEMS Microbiol Ecol* 2019a;**95**.

Sanyal SK, Shuster J, Reith F. Cycling of biogenic elements drives biogeochemical gold cycling. *Earth-Sci Rev* 2019b;**190**: 131-47.

Sanyal SK, Brugger J, Etschmann B et al. Metal resistant bacteria on gold particles: Implications of how anthropogenic contaminants could affect natural gold biogeochemical cycling. *Sci Total Environ* 2020;138698.

Schubert M, Lindgreen S, Orlando L. AdapterRemoval v2: rapid adapter trimming, identification, and read merging. *BMC Res Notes* 2016;**9**: 88.

Shuhong Y, Meiping Z, Hong Y *et al.* Biosorption of Cu^{2+}, Pb^{2+} and Cr^{6+} by a novel exopolysaccharide from *Arthrobacter* ps-5. *Carbohydr Polym* 2014;**101**: 50-6.

Shuster J, Bolin T, MacLean LC *et al.* The effect of iron-oxidising bacteria on the stability of gold (I) thiosulphate complex. *Chem Geol* 2014;**376**: 52-60.

Shuster J, Johnston CW, Magarvey NA *et al.* Structural and chemical characterization of placer gold grains: implications for bacterial contributions to grain formation. *Geomicrobiol J* 2015a;**32**: 158-69.

Shuster J, Marsden S, Maclean LC *et al.* The immobilization of gold from gold (III) chloride by a halophilic sulphate-reducing bacterial consortium. *Geological Society, London, Special Publications* 2015b;**393**: 249-63.

Shuster J, Reith F. Reflecting on Gold Geomicrobiology Research: Thoughts and Considerations for Future Endeavors. *Minerals* 2018;**8**: 401.

Shuster J, Reith F, Cornelis G *et al.* Secondary gold structures: Relics of past biogeochemical transformations and implications for colloidal gold dispersion in subtropical environments. *Cheml Geol* 2017;**450**: 154-64.

Song H-P, Li X-G, Sun J-S *et al.* Application of a magnetotactic bacterium, Stenotrophomonas sp. to the removal of Au (III) from contaminated wastewater with a magnetic separator. *Chemosphere* 2008;**72**: 616-21.

Southam G, Beveridge TJ. The in vitro formation of placer gold by bacteria. *Geochim Cosmochim Acta* 1994;**58**: 4527-30.

Srivastava S, Thakur IS. Biosorption and biotransformation of chromium by Serratia sp. isolated from tannery effluent. *Environ Technol* 2012;**33**: 113-22.

Staehlin BM, Gibbons JG, Rokas A et al. Evolution of a Heavy Metal Homeostasis/Resistance Island Reflects Increasing Copper Stress in Enterobacteria. *Genome Biol Evol* 2016;**8**: 811-26.

Stehouwer R, Day RL, Macneal KE. Nutrient and trace element leaching following mine reclamation with biosolids. *J Environ Qual* 2006;**35**: 1118-26.

Sultana M, Mou TJ, Sanyal SK et al. Investigation of Arsenotrophic Microbiome in Arsenic-Affected Bangladesh *Groundwater*. 2017;**55**: 736-46.

Tamura K, Dudley J, Nei M *et al.* MEGA4: molecular evolutionary genetics analysis (MEGA) software version 4.0. *Mol Biol Evol* 2007;**24**: 1596-9.

Teitzel GM, Parsek MR. Heavy metal resistance of biofilm and planktonic Pseudomonas aeruginosa. *Appl Environ Microbiol* 2003;**69**: 2313-20.

Tordoff G, Baker A, Willis A. Current approaches to the revegetation and reclamation of metalliferous mine wastes. *Chemosphere* 2000;**41**: 219-28.

Varol M, Şen B. Assessment of nutrient and heavy metal contamination in surface water and sediments of the upper Tigris River, Turkey. *Catena* 2012;**92**: 1-10.

Wang X, Preston JF, Romeo T. The *pgaABCD* locus of *Escherichia coli* promotes the synthesis of a polysaccharide adhesin required for biofilm formation. *J Bacteriol* 2004;**186**: 2724-34.

Wattam AR, Abraham D, Dalay O *et al.* PATRIC, the bacterial bioinformatics database and analysis resource. *Nucleic Acids Res* 2013;**42**: D581-D91.

Webb JS, Givskov M, Kjelleberg S. Bacterial biofilms: prokaryotic adventures in multicellularity. *Curr Opin Microbiol* 2003;**6**: 578-85.

Wick RR, Judd LM, Gorrie CL *et al.* Unicycler: resolving bacterial genome assemblies from short and long sequencing reads. *PLoS Comput Biol* 2017;**13**: e1005595.

Wiesemann N, Bütof L, Herzberg M *et al.* Synergistic toxicity of copper and gold compounds in *Cupriavidus metallidurans*. *Appl Environ Microbiol* 2017;**83**: e01679-17.

Wiesemann N, Mohr J, Grosse C *et al.* Influence of copper resistance determinants on gold transformation by *Cupriavidus metallidurans* strain CH34. *J Bacteriol* 2013;**195**: 2298-308.

Xu L, Dong Z, Fang L et al. OrthoVenn2: a web server for whole-genome comparison and annotation of orthologous clusters across multiple species. *Nucleic Acids Res* 2019;**47**: W52-W8.

Youngson J, Craw D. Gold nugget growth during tectonically induced sedimentary recycling, Otago, New Zealand. *Sediment Geol* 1993;**84**: 71-88.

Yung MC, Ma J, Salemi MR *et al.* Shotgun proteomic analysis unveils survival and detoxification strategies by *Caulobacter crescentus* during exposure to uranium, chromium, and cadmium. *J Proteome Res* 2014;**13**: 1833-47.

Zammit CM, Weiland F, Brugger J *et al.* Proteomic responses to gold (iii)-toxicity in the bacterium *Cupriavidus metallidurans* CH34. *Metallomics* 2016;**8**: 1204-16.

Figure 1

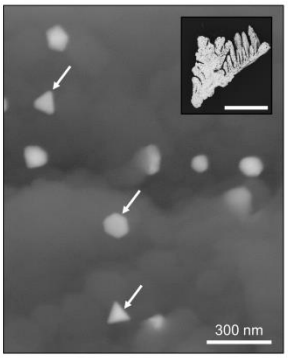

Figure 1. A low-magnification backscatter electron (BSE) scanning electron microscope (SEM) micrograph of a gold particle recovered from Donnybrook, Western Australia (inset). See Sanyal et al., 2019b for details on particle characterised. A low-magnification BSE SEM micrograph of pure gold nanoparticles that occur as octahedral platelets (arrows). These gold nanoparticles were closely associated with clay minerals and residual organic material within polymorphic layers.

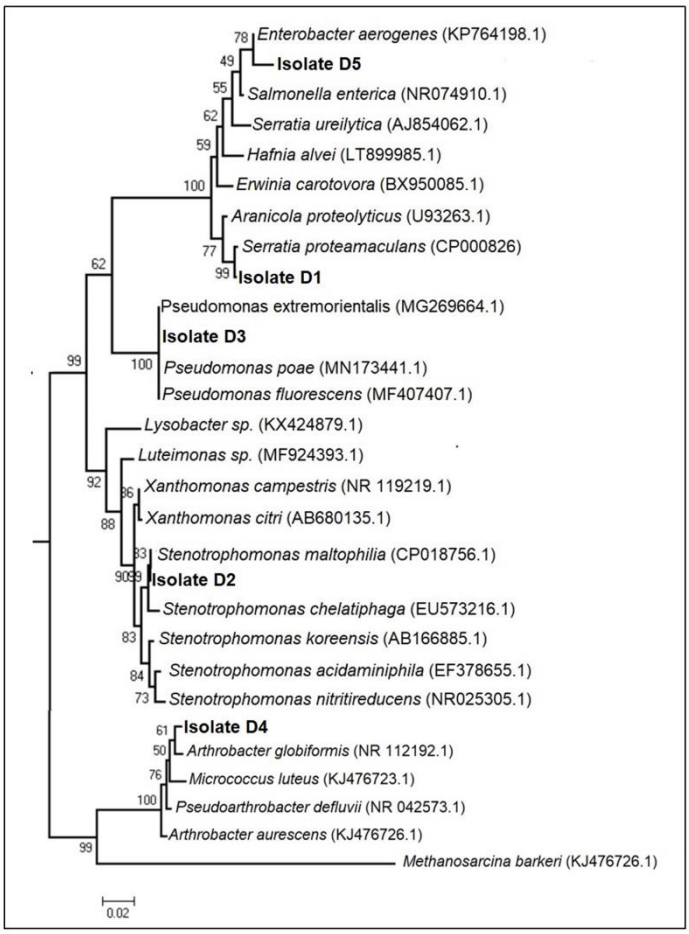

Figure 2. Neighbour-joining 16S rRNA tree showing the phylogenetic positions of the gold-tolerant bacteria that were isolated from the selective enrichment. Numbers at branching points indicate bootstrap values determined from 1000 iterations.

Figure 3

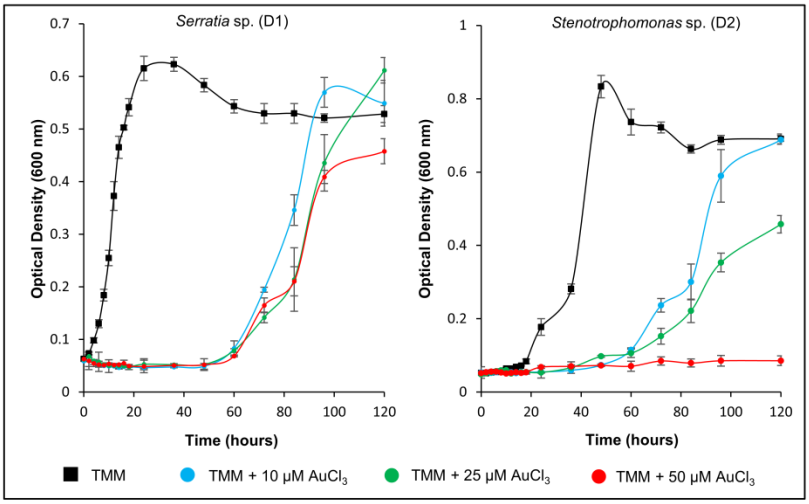

Figure 3. A graphical plot of *Serratia* sp. and *Stenotrophomonas* sp. growth patterns in the present of soluble $AuCl_3$ solutions.

Figure 4

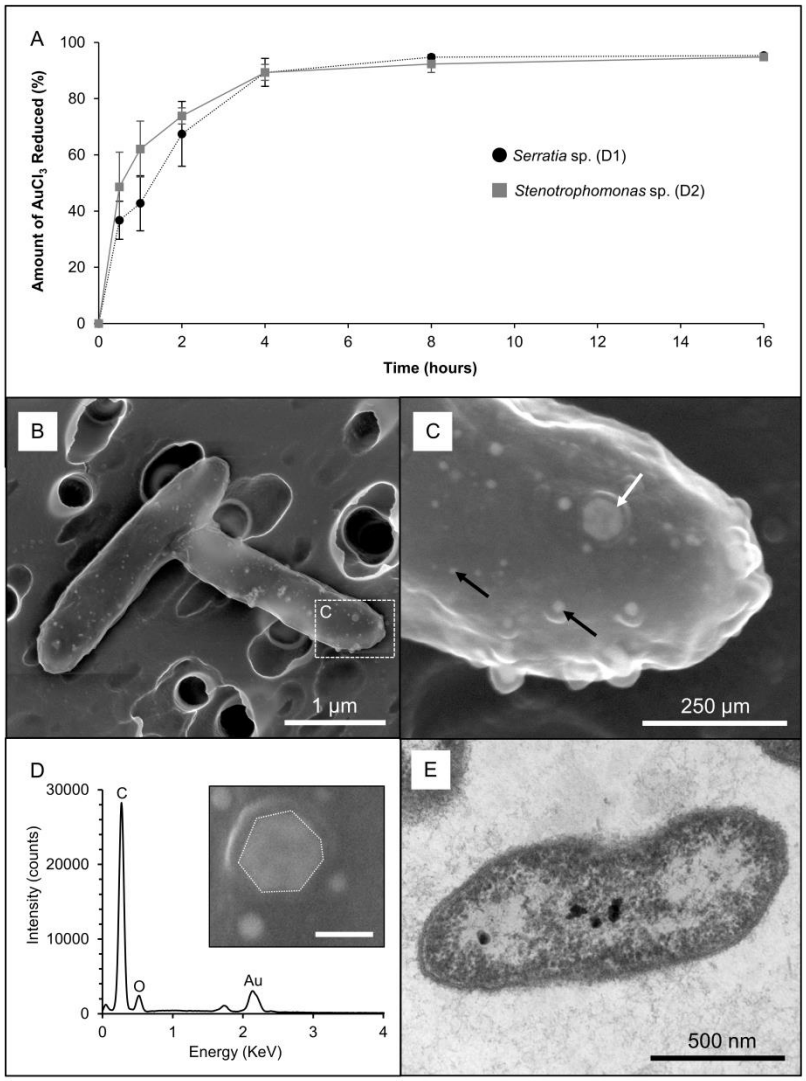

Figure 4. The graphical plot of $AuCl_3$ reduction by *Serratia* sp. and *Stenotrophomonas* sp. over time (A). A representative, low-magnification secondary electron (SE) SEM micrographs of *Serratia* sp. exposed to soluble gold for 2 hours. Cells were rod-shaped with gold nanoparticle occurring on the extracellular surface (B). A high-magnification SE SEM micrograph of gold nanoparticles (C, black arrows), some of which occurred as octahedral

platelets (C, white arrow). A representative energy dispersive spectroscopy (EDS) spectrum of the octahedral gold nanoparticles (D). Note the dashed line highlights the crystal boundaries (D, inset). A low-magnification TEM micrograph of *Serratia* sp. exposed to soluble gold for 2 hours. Ultrathin TEM sections revealed that soluble gold was also intracellularly reduced and occurred as nanoparticles less than 50 nm in size (E). Note that *Stenotrophomonas* sp. also reduced $AuCl_3$ as pure gold nanoparticles less than 100 nm in size both extracellularly and intracellularly (micrographs not shown).

Figure 5

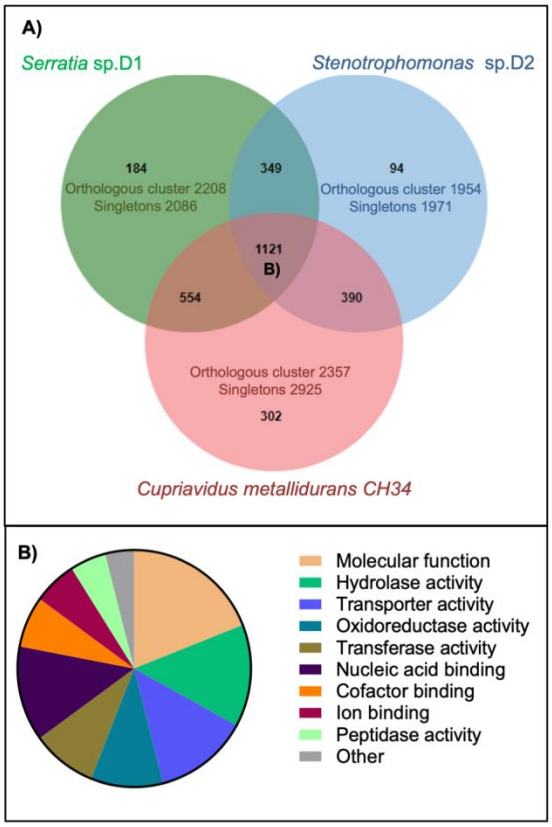

Figure 5. A Venn diagram showing the numbers of unique and shared orthologous genes clusters

among *Serratia* sp., *Stenotrophomonas* sp., and *Cupriavidus metallidurans* CH34 (A). A pie-chart showing the functional distributions of 1121 orthologous genes shared by all the three bacteria.

Figure 6

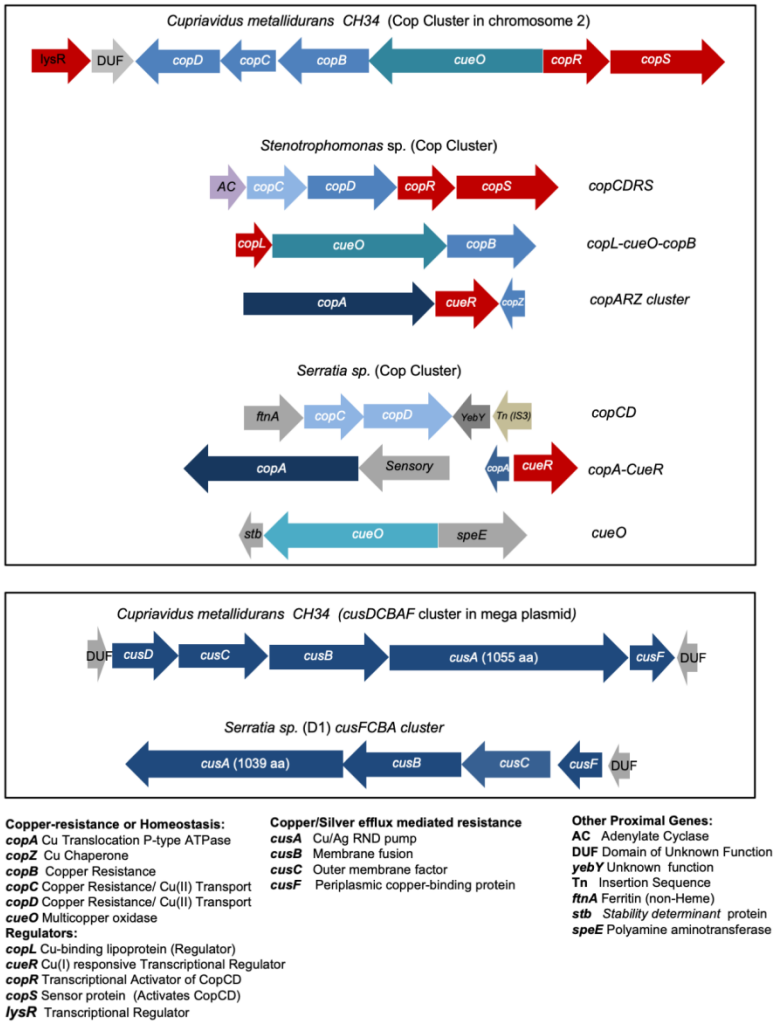

Copper-resistance or Homeostasis:
copA Cu Translocation P-type ATPase
copZ Cu Chaperone
copB Copper Resistance
copC Copper Resistance/ Cu(II) Transport
copD Copper Resistance/ Cu(II) Transport
cueO Multicopper oxidase
Regulators:
copL Cu-binding lipoprotein (Regulator)
cueR Cu(I) responsive Transcriptional Regulator
copR Transcriptional Activator of CopCD
copS Sensor protein (Activates CopCD)
lysR Transcriptional Regulator

Copper/Silver efflux mediated resistance
cusA Cu/Ag RND pump
cusB Membrane fusion
cusC Outer membrane factor
cusF Periplasmic copper-binding protein

Other Proximal Genes:
AC Adenylate Cyclase
DUF Domain of Unknown Function
yebY Unknown function
Tn Insertion Sequence
ftnA Ferritin (non-Heme)
stb *Stability determinant* protein
speE Polyamine aminotransferase

Figure 6. A schematic of different copper-resistance genes clusters (*cop*, *cus*, *cue*) either detected in *Serratia* sp. (D1) or *Stenotrophomonas* sp. (D2) and its comparison with *Cupriavidus metallidurans* CH34. The size of the arrow represents the relative length of the genes with in and between the organisms. The arrow with the same colour represents the significant sequence homology (>70%) of the genes.

Figure 7

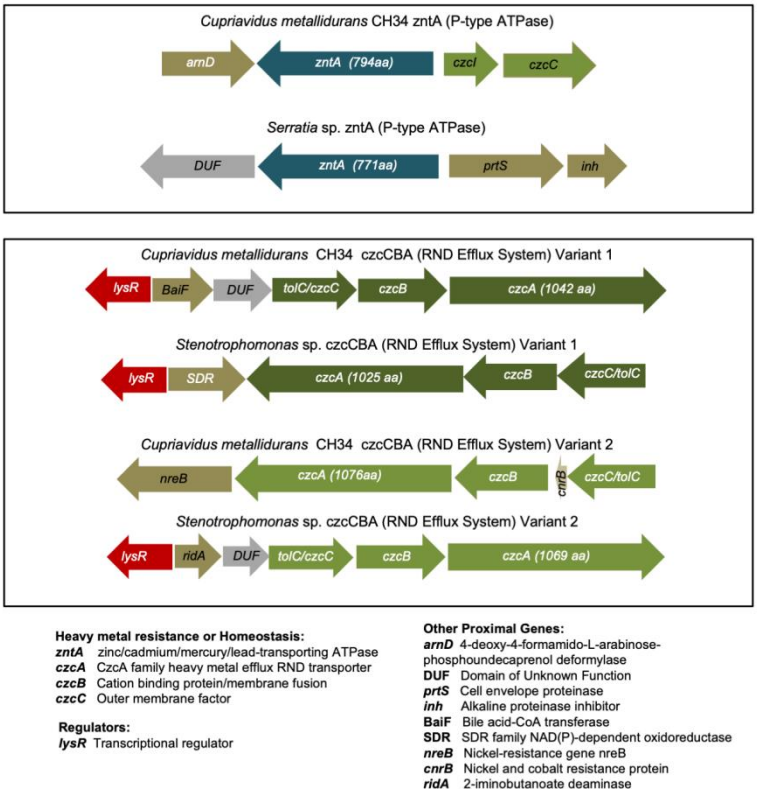

Figure 7. A schematic of different heavy-metal (e.g., lead, zinc, cobalt, cadmium) resistance gene clusters (*znt*, *czc*) either detected in *Serratia* sp. or *Stenotrophomonas* sp. and its comparison with *Cupriavidus metallidurans* CH34. The size of the arrow represents the relative length of the genes within and between the organisms. The arrow with the same colour represents the significant sequence homology (≥70%) of the genes.

Figure 8

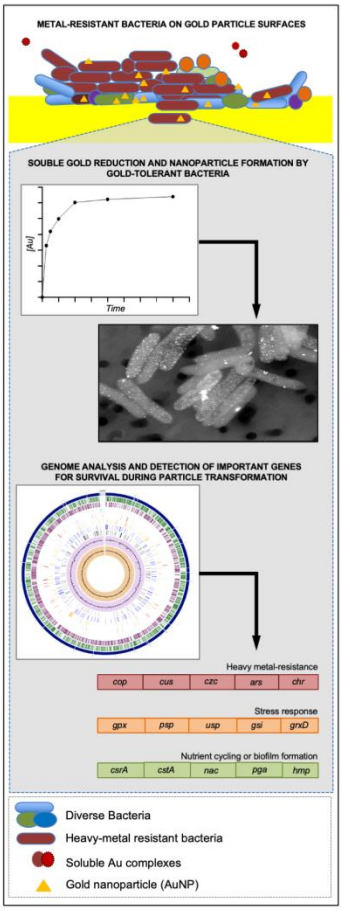

Figure 8. A schematic diagram representing Au-tolerant bacteria on gold particles and bacterial physiology and genomic capacity to survive Au biogeochemical cycling

Table 1. Comparison of general genome features from *Serratia* sp. (D1) and *Stenotrophomonas* (D2) and *C. metallidurans* CH34.

Genome Properties	*Serratia* sp.	*Stenotrophomonas* sp.	*C. metallidurans* CH34	
			CHR1	CHR2*
Genome Size (Mb)	5.2	4.6	3.93	2.58
G + C ratio (mol %)	54.9	66.04	63.8	63.6
Total Genes	4914	4293	3652	2314
Protein Coding Genes	4771	4176	3522	2256
tRNA	75	63	55	8
rRNA Genes	3	4	6	6
Genomic Island	6	9	11	0
Transposable Elements	12	14	8	7
Plasmid	0	0	2	

*Mega Plasmid

Table 2. The detection of heavy-metal resistance genes in *Serratia* sp. (D1), *Stenotrophomonas* sp. (D2), and *C. metallidurans* CH34.

Heavy-metal	Gene	Protein Name	Biological Function	D1	D2	CH34
Copper (Cu)	*copA*	Cu-translocating P-type ATPase	Detoxification of Cu ion	+	+	+
	copB	Cu resistance protein B	Cellular Cu ion homeostasis	-	+*	+*
	copC	Periplasmic Cu-binding protein	Cu ion transport	+	+*	+*
	copD	Cu-resistance membrane protein	Cu detoxification via transport	+	+*	+*
	copZ	Cu chaperone	Cu(I)-binding and delivery to CopA	-	+	+
	copL	Cu-binding lipoprotein (Regulator)	Cu hyper resistance	-	+	+
	cueO	Multicopper oxidase	Cu detoxification via Cu(I) oxidation	+	+	+
	cupC	Cytoplasmic Cu metallochaperone	Cupo-protein maturation	-	+	+
	cusA	Cu/Ag Efflux RND Transporter	Resistance to Cu and Ag	+*	-	+*
	cusB	Membrane fusion protein	Resistance to Cu and Ag	+*	-	+*
	cusC	Outer membrane efflux protein	Resistance to Cu and Ag	+*	-	+*
	cusF	Periplasmic Cu-binding protein	Resistance to Cu and Ag	+*	-	+*
Cobalt (Co) Zinc (Zn) Cadmium (Cd)	*zntA*	Zn/Cd/Co transporting ATPase	Heavy-metal resistance	+*	-	+*
	czcA	Metal cation efflux: RND Transporter	Heavy-metal resistance	-	+*	+*
	czcB	Metal cation efflux: membrane fusion protein	Heavy-metal resistance	-	+*	+*
	czcC	Outer membrane efflux protein	Heavy-metal resistance	-	+*	+*
Arsenic (As)	*arsB*	Arsenical pump membrane protein	As resistance via As (III) efflux	-	+*	+*
	arsC	Glutaredoxin-dependent arsenate reductase	As resistance via As(V) reduction	+*	+*	+
	arsC1	Arsenate reductase	As resistance via As(V) reduction	-	+	+
Chromium (Cr)	*chrA1, A2*	Chromate transport protein	Reduces chromate accumulation via transport	-	+	+

+ Detection
- No detection
*Significant sequence homology

Table 3. The detection of stress response, nutrient cycling, and biofilm formation genes in *Serratia* sp. (D1), *Stenotrophomonas* sp. (D2), and *C. metallidurans* CH34.

Trait	Gene	Protein Name	Biological Function	D1	D2	CH34
Stress Response	*gpx*	Glutathione peroxidase	Detoxification via free-radical neutralisation (H_2O_2 related)	+*	+*	+*
	gstA	Glutathione transferase	Detoxification via free-radical neutralisation (H_2O_2 related)	+*	+*	+*
	sodB	Superoxide dismutase	Removal of superoxide radicals	+*	+*	+*
	ohr	Organic hydroperoxide resistance	Neutralisation of oxidative stress	+*	+*	+*
	yggX	Fe(II)-trafficking protein	Cellular response to oxidative stress	+	+	+
	gsiBC	Glutathione ABC transporter	Oxidative stress neutralization due to heavy metal stress	+	-	-
	pspG	Envelope stress response protein	Reducing oxidative stress on cell membrane	+	-	-
	grx	Monothiol glutaredoxine	Protect against oxidative stress and maintain redox homeostasis	+	+	+
	glsB	Stress responsive membrane	Reducing oxidative stress on cell membrane	+	-	-
Nutrient Cycling	*csrA*	C storage regulation	Regulates carbohydrate metabolism under nutrient limiting condition	+*	+*	-
	cstA	C starvation	Peptide uptake in response to starvation	+*	+*	+*
	narK	Nitrate/nitrite transporter	Nitrate assimilation	+*	+*	+*
	ntrBC	N regulation	N fixation	+	-	+
	ntrY	N assimilation regulation	N fixation	-	+	+
	nac	N assimilation regulation	Regulates nitrogen metabolism in nitrogen limiting condition	-	+	-
	azoR	FMN-dependent NADH-azoreductase	Xenobiotic degradation via biotransformation	+	+	-
	-	Aromatic ring-hydroxylating dioxygenase	Xenobiotic degradation	+	+	-
Biofilm Formation	*hmpS*	Biofilm formation regulator	Intercellular signal transduction	+	-	-
	bsmA	Biofilm peroxide resistance protein	Acid and peroxide neutralisation	+	-	-
	pgaA BCD	poly-beta-1,6-N-acetyl-D-glucosamine	Biofilm matrix structural stability	-	+	-

+ Detection
- No detection
*Significant sequence homology